Applied Catalysis B: Environmental 218 (2017) 220–229

Contents lists available at ScienceDirect

Applied Catalysis B: Environmental

journal homepage: www.elsevier.com/locate/apcatb

Bio-adipic acid production by catalysed hydrogenation of muconic acid in mild operating conditions

S. Capelli[a,1], A. Rosengart[b,1], A. Villa[a], A. Citterio[b], A. Di Michele[c], C.L. Bianchi[a], L. Prati[a], C. Pirola[a,*]

[a] Dipartimento di Chimica, Università degli Studi di Milano, Via Golgi 19, 20133 Milano, Italy
[b] Department of Chemistry, Materials and Chemical Engineering "Giulio Natta", Politecnico di Milano, Via Mancinelli 7, 20133 Milano, Italy
[c] Dipartimento di Fisica e Geologia, Università degli Studi di Perugia, Via Ascoli 1, 06123 Perugia, Italy

ARTICLE INFO

Article history:
Received 20 April 2017
Received in revised form 15 June 2017
Accepted 20 June 2017
Available online 22 June 2017

Keywords:
Muconic acid
Hydrogenation
Bio-adipic acid
Heterogeneous catalysis
Platinum

ABSTRACT

In this work *trans,trans*-muconic acid was hydrogenated to adipic acid, a strategic intermediate for the industry of polyamides and high performance polymers. This study: (1) develops a new and robust analytical method for the evaluation of muconic acid conversion and adipic acid selectivity, (2) defines a standard procedure for the confirmation of the kinetic regime using experimental data and some practical criteria to exclude mass transfer limitations, (3) tests Pt/C 5% commercial catalyst for the study of muconic acid hydrogenation at different operating conditions, (4) hypothesizes a reaction pathway in aqueous media, and (5) demonstrates the possibility to recycle the catalyst without loss in activity and selectivity. The developed analytical method evaluates muconic acid conversion by UV–vis analyses, while the selectivity towards adipic acid and mono-unsatured intermediates was determined by GC/TCD analysis after derivatization of the reaction mixture. Under optimized conditions the hydrogenation reaction (70 °C, 4 bar of hydrogen and 10 substrate/catalyst ratio (wt/wt)) reached full conversion with full selectivity toward adipic acid in 2 h. Finally, recycling tests revealed the possibility to reuse catalyst up to 10 times without loss in conversion and selectivity opening the way to a scaling up of the process.
© 2017 Elsevier B.V. All rights reserved.

1. Introduction

Climate change, limited oil reserves and geopolitical concerns combine to motivate an urgent quest for alternatives to fossil derived fuels and commodity chemicals (the Grand Challenges). In this sense, industrial innovation has already accepted the responsible practice of low energy use and minimal waste generation, to align economic and environmental sustainability. As a further step, a growing number of chemical industries are developing alternative processes that are based on renewable sources. Much effort in this direction has been done for the development of a bio-based adipic acid production. Adipic acid (AA) is a strategic commodity chemical, widely used as monomer in the synthesis of polyamides (PA-6,6), polyesters and other specialty products: PA-6,6 accounts for about 85% of the total adipic acid demand, while other relevant applications are polyurethanes (5%), and adipic esters (4%) [1]. Global adipic acid annual demand was estimated at 2.3 million metric tons in 2012 with a growth rate of 3–5% per year [2]. So far, the totality of the commercialized adipic acid derives from oil, mostly from the relatively expensive benzene fraction [3].

In spite of more than five decades of optimization, the traditional process for AA (known as the "KA-oil process") still raises great environmental and safety concerns. The stocks of dangerous and volatile reactants (benzene and ammonia), the explosion hazard due to peroxides formation and hexane instability, the production of great amounts of greenhouse gases from the nitric acid oxidation [4] are only some of the downsides of the oil-based technology.

For these reasons, research and industry have started to look at alternative solutions since early 1990s, and today a consistent amount of patents and publications has been accumulated, exploring chemical and biochemical transformations, that consider different feedstock and process scenarios [5,6]. In particular, one of the most promising green routes is based on the production of adipic acid from *cis,cis*-(2Z,4Z) muconic acid (MA), a bio-derived platform chemical, that can be obtained from both lignin and carbohydrate fraction of lignocellulosic biomass [7], the most abundant renewable material on Earth. Biological production of *cis,cis*-MA has been extensively studied, leading to the development of several engineered strains able to produce the diacid following two

* Corresponding author.
E-mail address: carlo.pirola@unimi.it (C. Pirola).
[1] These authors have equally contributed to the present work.

http://dx.doi.org/10.1016/j.apcatb.2017.06.060
0926-3373/© 2017 Elsevier B.V. All rights reserved.

Nomenclature

a_p	External surface area of the catalyst per unit volume ($m^2\ m^{-3}$)
C^*H_2	Concentration of hydrogen in equilibrium with the liquid phase ($kmol\ m^{-3}$)
C_i	Concentration of species i ($kmol\ m^{-3}$)
d_p	Particle diameter (m)
D_{H_2}	Molecular diffusivity ($m^2\ s^{-1}$)
$k_l a_B$	Gas to liquid mass-transfer coefficient (s^{-1})
k_s	Liquid to solid mass-transfer coefficient (s^{-1})
l	Impeller diameter (m)
n	Rotation speed (rps)
r	Radius of the catalyst pellet (m)
R_A	Overall rate of hydrogenation ($kmol\ m^{-3}\ s^{-1}$)
V	Liquid volume (m^3)
W	Catalyst weight ($kg\ m^{-3}$)
α_1	Parameter defined by Eq. (2)
α_2	Parameter defined by Eq. (3)
μ_l	Viscosity of the liquid (P)
ρ_l	Density of liquid ($kg\ m^{-3}$)

major strategies: (1) a direct bio-synthesis from glucose via the pentose cycle [8] (2) a metabolic transformation of aromatics (such as benzoate, toluene, benzene, phenol, aniline, and salicylate) via the catechol *ortho*-cleavage pathway [9–11].

New interesting applications are stimulating further the research toward the scale-up of MA fermentations. For example, the recently disclosed syntheses of industrially relevant monomers from MA as diethyl terephtatalate [12] and 1,4-cyclohexanedicarboxylic acid [13], or the employment of MA isomers to the development of new high-performance unsaturated polyesters (UPE) [14,15].

With regard to the hydrogenation of MA to achieve AA, innovative and promising technologies have been recently disclosed, in particular some electrocatalytic membrane reactors that not only are effective in presence of the fermentation impurities [16], but also allow to produce the monounsaturated 3 hexenedioic acid, employed to produce unsaturated polyamides [17]. On a shorter time horizon though, a catalytic hydrogenation of MA to AA is an easier-to-industrialize solution, given the maturity of this hydrogenation technology. However, this step risks becoming a major bottleneck, without an improvement of the present reaction yields and conversion, optimizing the reaction conditions.

The scientific literature published so far addressed MA hydrogenation with the main purpose of proving the feasibility of the reaction, rather than achieving good performances in scalable conditions (low temperature and pressure, stable catalysts and environmental friendly solvents) [3,14,18–22]. Focusing on some of the most recent papers, Thomas et al. tested Pt/SiO_2 1% at 80 °C and 30 bar of hydrogen in ethanol; 100% conversion muconic acid was obtained after 5 h with a selectivity toward AA at about 90% [19].

The hydrogenation in ethanol was further improved obtaining good yield (>90%) within 35 min at room temperature using commercial Pt/AC 5% catalyst at 24 bar of hydrogen pressure [23].

Previously, different supported Rh catalysts were tested for MA hydrogenation as well, obtaining fairly good selectivity (>90%) and conversion (>95) in 5 h, but requiring 69 bar of pressure, high temperature (210 °C), and a toxic solvent as methanol [24].

As for non-noble metal catalysts, Scelfo et al., 2016 succeeded in hydrogenating MA on 14.2% Ni/Al_2O_3 catalyst, with complete selectivity to AA in 5 h, at only 60 °C in water. Still, the reaction required 5 h and 10 bar of H_2 pressure [25]. For safety and cost reasons, it would be advisable to achieve the same results at lower pressures, possibly in a shorter period of time.

Another aspect worth of consideration is that mostly *cis,cis*-MA has been investigated for the hydrogenation, without considering that *cis,cis* isomer is the most instable and spontaneously evolves into the geometrical isomer *cis,trans* in acidic environment at temperatures above 30 °C [16].

Also, it has been extensively proven that both *cis,cis* and *cis,trans*-MA tend to isomerize to *trans,trans*-MA in the presence of metals that strongly bind hydrogen molecules [16,20,21].

It is therefore particularly important to consider the most plausible downstream operations on the fermentation broth before the hydrogenation step, at least on a first approximation. An example of the broth workup can be found in [23], where it is evident, already at lab scale, that the filtered broth undergoes to a crystallization step achieved by pH shift: the acid form is less soluble that muconate salts. Moreover, in a full-scale bioprocess, an increase of temperature above 80 °C is often required for bacteria deactivation, and even in presence of thermo-labile compounds, a concentration step is required to enhance product recovery [26]. The coupled conditions of acidic environment and higher temperatures are therefore a realistic scenario, and the *cis,cis* form is unlikely to be preserved: the hydrogenation will be possibly performed on a mixture of the three isomers. As for the presence of lactons, a shorter treatment could avoid this occurrence [13].

Therefore, we selected *trans,trans* MA as the best chemical model for the hydrogenation study, as it is the most stable and less soluble isomer. The optimal reaction conditions for the *trans,trans* form can be applied readily to the other isomers, in virtue of their lower activation energy [16]. Also, in the perspective of a future kinetic study, *trans,trans*-MA allows removing all the isomerization reactions from the system.

This work examines the catalytic hydrogenation using a model solution of water, in a batch reactor using a commercial Pt/C (5% wt/wt loading) heterogeneous catalyst. To enhance the reaction velocity, we decided to investigate Pt/C catalyst as previously done by Niu [3], increasing the temperature from the original 24 °C up to 70 °C. Other variables that more negatively affect the process economics were considered, as the amount of noble metal and the pressure. The conversion, yield and selectivity were evaluated setting up a suitable and robust gas-chromatographic analytical method, differently from the liquid ones develop by Carraher et al. [27], and all by-products were identified. The choice of using water as reaction medium was determined by its minimal environmental impact and because several authors have mentioned the possibility to perform the hydrogenation directly in the M9 culture media on the salt form of MA [7]. On this latter aspect, we included an evaluation of the performance of the hydrogenation catalyst in conditions that reproduce a possible industrial substrate, i.e. a pre-purified fermentation broth containing muconic acid in the *cis,cis* form, in presence of some biological buffer salts. In this way, a first insight on the global downstream strategy can be provided, on an integrated process development approach.

2. Experimental

2.1. Materials

Pt/C 5% loading was purchased from Sigma Aldrich n.v. *trans,trans*-muconic acid (98%), *cis,cis*-muconic acid (97%), sodium phosphate dibasic (>99.5%), potassium phosphate monobasic (>98%), sodium chloride (>99%), dimethyl 2,4-hexadiene-1,6-dioate (>99%), dimethyl (3E)-3-hexenedioate (>99%), methanol (99.8%), butanol (>99%), sulphuric acid (98%), sodium hydroxide, adipic acid (>99%), (2E)-2-hexenedioic acid (*trans*,beta hydromu-

conic acid) (98%) and dimethyl adipate (≥99%) were purchased from Sigma Aldrich.

2.2. Catalyst characterization

TPD/R/O 1100 ThermoQuest Instruments was used for TPR study. An amount 40 mg of catalyst was dried in oven and then analysed. The sample was pre-treated with argon flow from room temperature to 200 °C with a temperature ramp of 30 °C min^{-1} and maintained at this temperature for 60 min. The analysis was then conducted from 50 °C to 900 °C at 8 °C min^{-1} at 1 bar. The gaseous mixture was 5.04% of hydrogen in argon and it was fluxed within the instrument at 14 mL min^{-1}.

The BET surface areas of the as-purchased Pt/C 5% were determined using Sorptometer 1042 Costech.

SEM images were obtained using a Field Emission Gun Electron Scanning Microscopy LEO 1525 (ZEISS).The samples were investigated by Inlens detector for secondary electrons, AsB detector for backscattered electrons and elemental composition was determined using a Bruker Quantax EDS.

TEM images were obtained using a Philips 208 Transmission Electron Microscope.

2.3. Hydrogenation reaction

The hydrogenation reactions were carried out in an autoclave equipped with a thermocouple and a barometer for temperature and pressure control, respectively. The hydrogen and helium entered the reactor through the same line; helium is required to quench the reaction. The other line was used to introduce sodium muconate solution, avoiding any contamination with air, since trace oxygen may oxidize the reduced Pt. The reaction occurred in a glass cylindrical tube placed inside the stainless steel reactor to avoid that the Ni traces presents in the steel could invalidate the results due to its catalytic activity. Pt/C 5% (0.01–0.1 g) was reduced for 3 h at 200 °C under 6 bar of static hydrogen within the cylindrical glass tube, following the indication of the TPR analysis conducted on the fresh catalyst. The temperature was maintained constant trough a heating external metal jacket. After cooling, 10 mL of degassed muconate solution (0.07 M) were added to the reactor. The batch hydrogenations were conducted at 50 °C, 60 °C and 70 °C at 4 bar of static hydrogen with a magnetic stirring of 500 rpm up to 4 h.

Finally, an experimental campaign was conducted at 70 °C, 4 bar of hydrogen and 500 rpm on *cis,cis*-MA using a synthetic salt solution which reproduces a clarified fermentation broth as the one of Niu et al. [3]. This test considers the possibility to avoid a MA crystallization step before hydrogenation reaction, preventing the solution acidification and the risk of MA isomerization. The synthetic fermentation broth contained *cis,cis*-muconic acid (28 g/L), Na_2HPO_4 (50 g/L), KH_2PO_4 (15 g/L), NaCl (2.5 g/L) and NaOH (40 g/L).

After every reaction, the catalyst was removed by filtration and the solution analysed as described in 2.4. The filtrate was analysed by ICP-OES to check for metal leaching.

2.4. Analytical procedure for conversion and selectivity evaluation

The conversion of the *trans,trans*-sodium muconate salt was evaluated by UV–vis analysis. After the catalyst filtration, the solution was analysed in a spectrophotometer T60 UV–vis Spectrophotometer PRIXMA from 400 to 190 nm. The maximum absorption was at 264 nm while at 210 nm a peak of intermediates was detected. The calibration of the analysis was performed with *trans,trans*-sodium muconate prepared starting from *trans,trans*-MA. No isomerization of *trans,trans*-MA was observed during the salification process.

The selectivity was estimated by gas chromatographic analyses on corresponding methyl esters following the experimental work validated by Vardon et al. [7].

The filtered samples were dried in oven at 70 °C. The white solid residues were reacted with methanol (7 mL) in large excess and sulphuric acid (50 μL) and left at slow stirring at 70 °C for 48 h. Different esterifications were then performed on pure *trans,trans*-MA, AA, and monounsatured compounds to verify if the acidic environment could influence the isomers distribution. Since MA esterification was not complete under the esterification conditions, it was not possible to evaluate the hydrogenation conversion of this compound using GC-TCD analyses: the UV–vis spectrophotometer was therefore employed.

Methyl esters were analysed by GC (Master GC Fast Gas Cromatograph Dani Instrument) equipped with TCD detector operating in split mode (1:3). Butanol was used as internal standard. The GC was outfitted with an Aldrich Supelcowax 10 (60 m × 0.53 mm id, 1 μL), and helium (15 mL min^{-1} column flow) was used as carrier at 5 mL min^{-1} flow rate. The GC-TCD method consisted of an inlet temperature of 210 °C and TCD transfer line at 240 °C. A starting temperature of 60 °C was set and then ramped at 18 °C min^{-1} to a temperature of 120 °C. Then from 120 °C to 160 °C ramped at 20 °C min^{-1}. From 160 °C to 260 °C the temperature increased at 15 °C min^{-1} and held for 1 min to purge the column. Dimethyladipate (DMA), dimethyl 2,4-hexadiene-1,6-dioate, and dimethyl-*trans*-β-hydromuconate synthesized from *trans*-β-hydromuconic acid were used for the instrument calibration, using butanol as internal standard. The recognition of the reaction intermediates was performed with GC coupled with mass detector (TraceISQ QD Single Quadrupole GC–MS) on the corresponding products. The inlet temperature was 280 °C and scan ranged from 50 *m/z* from 400 *m/z*. The temperature ramp was the same adopted for the GC-TCD analysis and the helium flow was 10 mL min^{-1} with a split ratio of 20. For a further control, dimethyl 2,4-hexadiene-1,6-dioate (by Sigma Aldrich) was injected to verify retention time, while dimethyl (3E)-3-hexenedioate standards was used to evaluate *trans,trans*-MA esterification.

3. Results and discussion

3.1. Analytical method

A suitable and robust analytical method was developed to control the reaction progress. Several complications were evidenced in previous studies of MA hydrogenation, especially from the analytical point of view [25]. GC analysis has been settled by transforming the reaction products into the corresponding esters by the method reported in 2.4. Unfortunately the esterification procedure was not quantitative for *trans,trans*-MA even after 48 h, most probably because of its low solubility. The calibration curves of the intermediates were obtained esterifying the corresponding commercial acid and checking their quantitative conversion by H NMR analysis. The conversion of *trans,trans*-MA was then followed by UV–vis analysis.

The intermediates of the hydrogenation reaction were recognized using GC–MS analysis. Fig. 1 shows a typical chromatogram obtained by GC-TCD. The developed method was able to determine and separate properly all the intermediates of the reacting mixture, distinguishing also the monounsaturated compounds *cis*-(Z)-2-hexenedioic acid (corresponding to peak b in Fig. 1) and the *trans*-(E)-2-hexenedioic acid (corresponding to peak c in Fig. 1). Since the *cis* intermediate is not commercially available, analy-

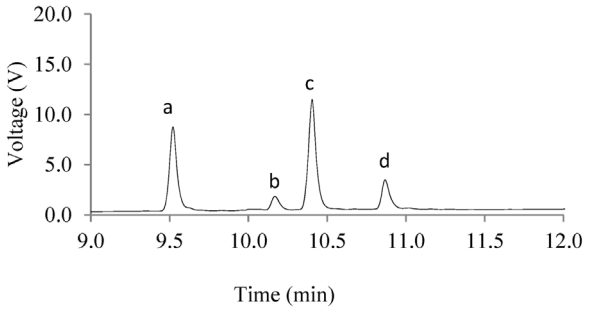

Fig. 1. GC-TCD chromatogram obtained with the developed analytical method. a) dimethyladipate b) (Z)-2-hexenedioic acid, c) (E)-2-hexenedioic acid and d) dimethylmuconate.

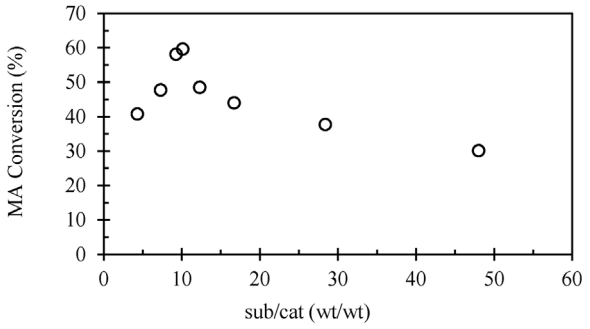

Fig. 2. Conversion evaluation at different substrate/catalyst ratio and at 60 °C, stirring = 500 rpm, P(H_2) = 4 bar, [MA] = $7 \cdot 10^{-2}$ M.

sis calibration toward this compound was performed with the response factor of the *trans* intermediate, given their similarity.

3.2. Evaluation of mass-liquid transfer phenomena

Initially, different tests at varied substrate/catalyst ratio were performed keeping constant temperature (40 °C), hydrogen pressure (4 bar) and reaction time (60 min), to select the best amount of catalyst.

The results reported in Fig. 2 show that, for a substrate/catalyst ratio equal to 10 (wt/wt), the reaction has the highest conversion, with good selectivity (65%).

An aspect that could significantly affect the performance of a slurry reactor is the insurgence of mass-transfer resistances between the gas (hydrogen), the liquid (water and reactants dissolved) and the solid (catalyst particles) phase. Although slurry reactors usually minimize transport phenomena issues, the confirmation of a pure kinetic regime is necessary if the reactor layout and the results are meant for further mechanism studies. Some practical criteria to exclude mass transfer resistances were presented by Chaudari and Rajashekharam [28–30]. They proposed qualitative indexes to assess whether any external or intraparticle mass transfer phenomena are the rate determining step, rather than the reaction itself. The values of the parameters cited below are reported in Table 1.

The calculation is based on the definition of initial rate, defined as:

$$R_A = \lim_{t \to 0} \frac{1}{\nu_i} \frac{dC_i}{dt} \quad (1)$$

where C_i is the concentration of a reference specie, in this case MA. The calculated value is of the order of 1.26 kmol/m^3/s.

Table 1
Different parameters used for evaluation of mass transfer phenomena.

Reaction conditions	
Hydrogen pressure	4 bar
Hydrogen gas-liq. transf. rate ($k_l a_B$)	0.1 s^{-1}
Liquid density	1000 kg m^{-3}
Liquid viscosity	6.5×10^{-4} Pa s
Reactor properties	
Volume	0.025 L
Reactor materials	glass
Impeller power number	5
Diameter of the impeller	2.5 mm
Rotation speed	8.33 rps
Catalyst properties	
Support	Activated charcoal
Pt content	5% wt/wt
Catalyst loading	10 $g_{cat} \cdot (L_{AM\ solution})^{-1}$
Catalyst porosity	0.95
Particle diameter	40×10^{-6} m
Particle skeletal density	2×10^3 kg m^{-3}

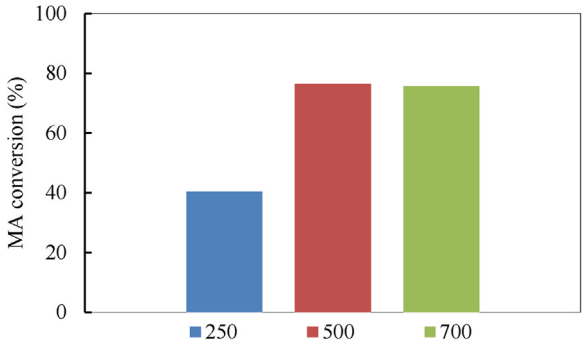

Fig. 3. Sodium *trans,trans*-muconate conversion evaluation at 250, 500 and 700 rpm T = 60 °C, P(H_2) = 4 bar, reaction time = 60 min, sub/cat = 10 (wt/wt) and [MA] = $7 \cdot 10^{-2}$ M.

The contribution of gas-liquid mass transfer is evaluated by the index defined in Eq. (2), which should be lower than 0.1 to exclude its contribution to the overall kinetics.

$$\alpha_1 = \frac{R_A}{k_l a_B C^*_{H_2}} < 0.1 \quad (2)$$

where $k_l a_B$ is the overall mass transfer coefficient (gas side-film theory) for stirred reactors, and $C^*_{H_2}$ is the equilibrium concentration of hydrogen. Machado [31] addressed the problem of estimating the gas-liquid mass transfer coefficient for bench-scale stirred reactors. The range of 0.05–0.5 s^{-1} was considered representative for the smaller hydrogenation reactors. Even with the more conservative values, the system under study resulted in α_1 values lower than 0.05. The calculated value is 0.03 that is safely under the threshold to exclude gas-liquid resistance.

Liquid-liquid mass transfer limitation was excluded performing a series of hydrogenations under the same conditions but varying the stirring speed from 250 to 700 rpm. The essays revealed that for higher speed than 500 rpm the system is no more sensitive to stirring, hence no more liquid-liquid transport is relevant on the overall kinetics (Fig. 3): the reactor can be considered a CSTR, therefore the hydrogen concentration in liquid bulk is assumed constant [32].

Liquid-solid mass transfer can be assessed by the index in Eq. (3).

$$\alpha_2 = \frac{R_A}{k_s a_p C^*_{H_2}} < 0.1 \quad (3)$$

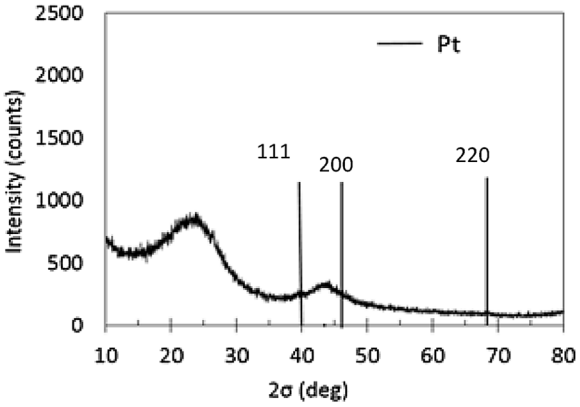

Fig. 4. XRPD diffraction spectrum on commercial Pt/C 5%.

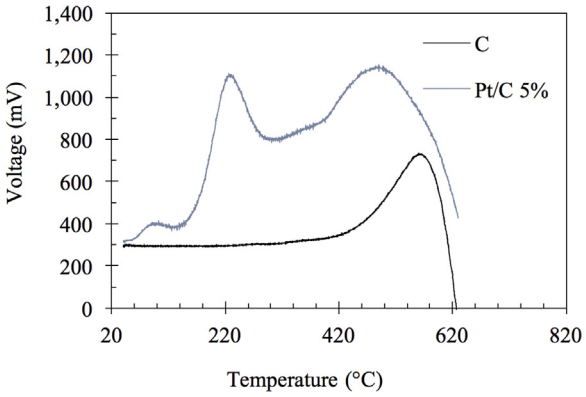

Fig. 5. TPR analysis of the commercial Pt/C 5%.

where k_s is the liquid-solid mass transfer coefficient, a_p is the interface area of liquid-solid boundary. The latter is defined by Eq. (4):

$$a_p = \frac{6w}{\rho_p d_p} \tag{4}$$

where w is the catalyst load, ρ_P and d_P are particle density and diameter respectively. Particles diameter was set using sieves and it was at about 40 μm (325 and 400 mesh −TYLER series)

The parameter k_s is obtained using a literature correlation [33]:

$$\frac{k_s d_p}{D_{H_2} F_c} = 2 + 0.4\left(\frac{d_p^4 \rho_l^3 e}{\mu_l^3}\right)^{0.25}\left(\frac{\mu_l}{\rho_l D_{H_2}}\right)^{0.33} \tag{5}$$

where D_{H_2} is the molecular diffusion of hydrogen in water, F_c is a shape factor assumed to be 1 for spherical particles, μ_l and ρ_l stand for liquid viscosity and density respectively, e is the energy supplied to the liquid by the stirrer, given in Eq. (6):

$$e = \frac{N_p n^5 l^5}{V} \tag{6}$$

where N_p is the impeller power number, l is the impeller diameter, n is the rotation speed (in rps). The calculated value for α_2 is 0.019, which allows excluding liquid-solid mass transfer limitations.

Finally, pore diffusion can be considered negligible if the parameter φ_{exp} is lower than 0.2:

$$\Phi_{exp} = d_p\left(\frac{\rho_P R_A}{w D_e c^*_{H2}}\right)^{0.5} < 0.2$$

where d_p is the particle diameter, w is the catalyst load, D_e is the effective diffusivity calculated as

$$D_e = \frac{D\varepsilon}{\tau}$$

where ε is the catalyst porosity and τ is the tortuosity factor. The latter parameter is usually little characterized: it is a complex function of the type of charcoal, of the adsorbed substrate, and the reaction medium, often regressed from indirect diffusion measurements [34]. Nonetheless, in Carbon-supported platinum hydrogenation catalysts, the parameter was estimated in the range between 3 and 7 [35].

The calculated φ_{exp} was lower than 0.04 even for the most conservative values of tortuosity in the conditions of this study, allowing the exclusion of pore diffusion mass transfer.

3.3. Catalyst characterization

The commercial Pt/C 5% used in our tests was by Sigma Aldrich.

The XRPD analysis (Fig. 4) shows the presence of very small crystal domains (<10 nm) of Pt (Sherrer equation). The surface area was first evaluated with BET method and for the fresh catalyst it is 1692 $m^2 g^{-1}$. The hydrogenation reaction was performed pretreating the catalyst in the same reactor at 200 °C in H_2.

TPR analysis (Fig. 5) shows that the reduction temperature of Pt surface oxide is near 220 °C (upper line). An additional peak at about 600 °C was addressed to the Carbon support. The slight shift to lower temperature of this latter peak observed in the Pt/C 5% compared to bare support (bottom line) was probably due to the catalytic effect of Pt which facilitates carbon reduction. A pre-reduction of catalyst was then performed under H_2 at 220 °C temperature.

TEM analysis of the fresh and used catalysts are reported in Fig. 6A and B, respectively. The fresh catalyst is characterized by a homogeneous distribution of Pt aggregates (black colour) on the carbon surface (grey colour). The size of these Pt aggregates can be estimated of about 4 nanometers. The situation is different in the sample after the pre-activation procedure and the reaction. In fact, in Fig. 6B it is possible to observe three times greater Pt particles than the corresponding ones present in the fresh sample. This result can be explained considering a sintering of Pt particle after pre-treatment step.

SEM analysis on fresh and used catalyst are reported in Fig. 7, where two different particles of the same sample were analysed, i.e. A) and B) for fresh catalyst and C) and D) for the used one. Images A) and C) were collected using secondary electron detectors, while B) and D) using backscattered electrons detector. By making a comparison between the different zones it is possible to conclude that the catalyst is homogeneous for what concerns both its morphology and Pt distribution. Moreover, SEM confirms the same observation previously discussed on the basis of TEM analysis.

EDX analysis reported in Fig. 8 show for fresh catalyst (Fig. 8A) a good dispersion of Pt on the surface of carbon support, while after reaction (Fig. 8B) Pt particle was less dispersed. In Fig. 8C and D the catalyst composition in fresh and used catalyst is reported. While in the fresh sample it is possible to confirm the theoretical catalyst composition, in the used sample sodium element was detected (Fig. 8D), due to the adsorption of sodium hydroxide used for muconic acid salification.

3.4. Batch hydrogenation of muconic acid

The hydrogenation tests were carried out in the batch reactor investigating different temperatures, as reported in Fig. 9.

It is clear that a complete conversion was achieved only at temperatures higher than 40 °C. At 70 °C, instead, the reaction was complete in only 1 h, while lowering the temperature to 50 °C allowed a complete conversion in 90 min. Considering the very low hydrogen pressure (4 bar), this catalyst has good performances compared to the Ni based ones and the Pt previously mentioned

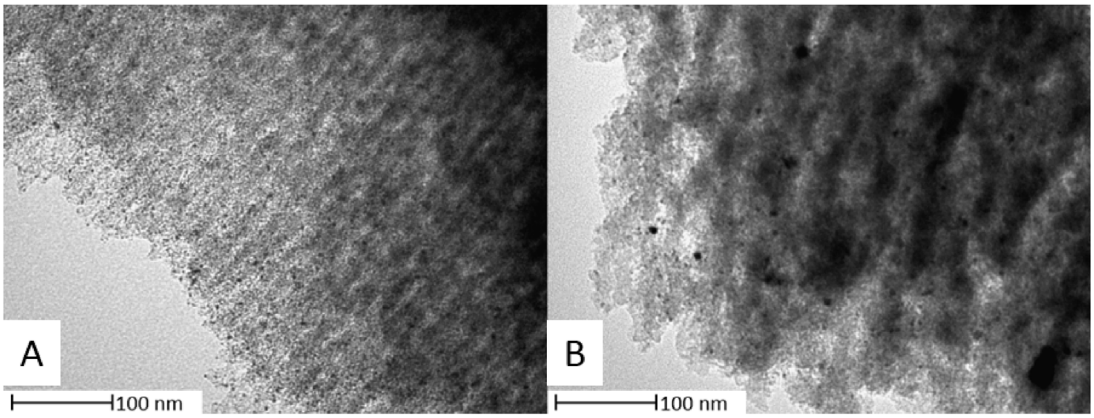

Fig. 6. Characterization by TEM of A) fresh and B) used catalyst.

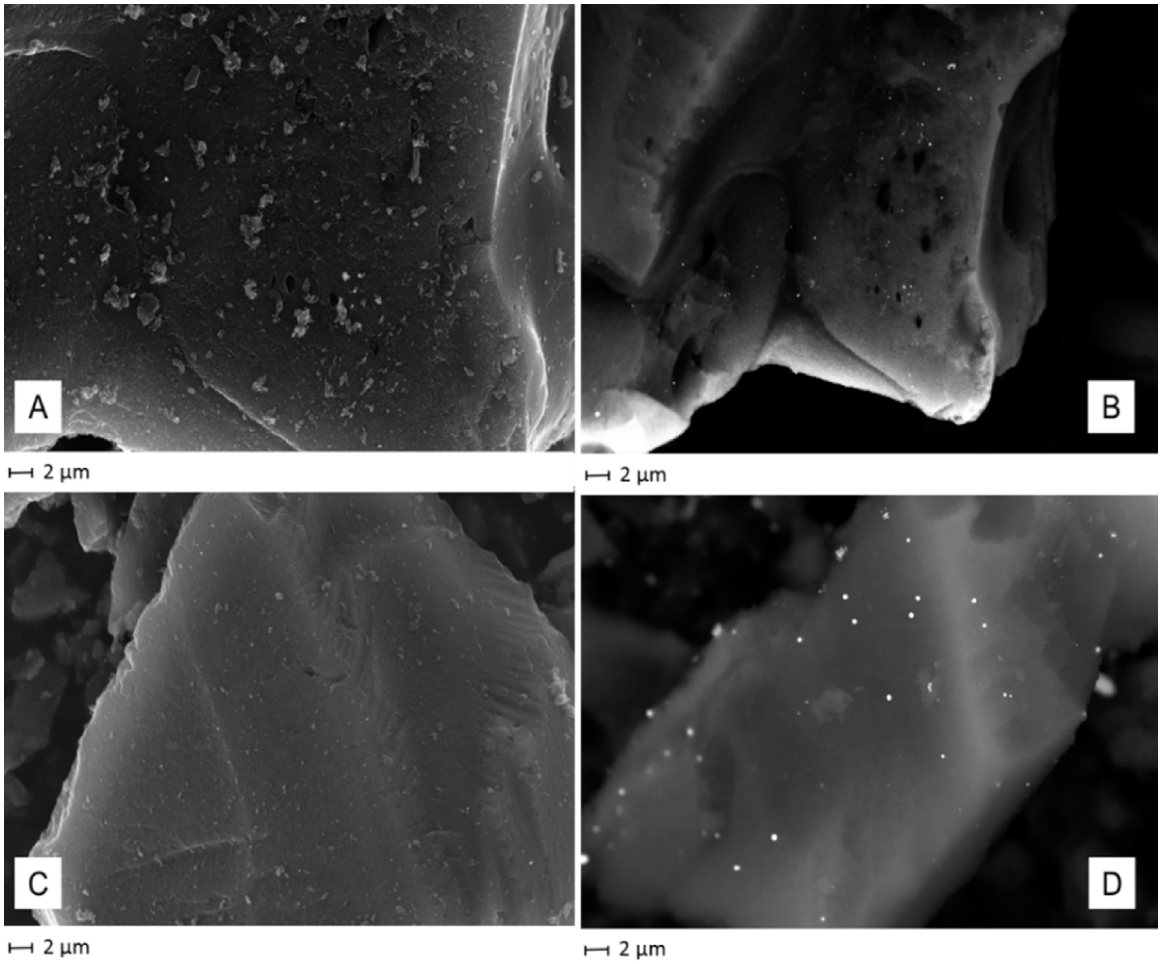

Fig. 7. Characterization by SEM of fresh (A, B) and used catalyst (C, D) in different zones.

[3,25]. Another remarkable aspect is that no metal leaching was observed after hot filtration thus confirming the heterogeneous behaviour of the reaction. For this experiment, the catalyst was filtered off after 1 h and the solution was allowed to be hydrogenated for other 2 h under the same operating conditions. No further conversion of MA was observed. Moreover, ICP analysis on the reaction media did not reveal the presence of metal, excluding leaching phenomena.

At 40 °C the catalyst seemed to slowly deactivate at about 90% of conversion. The reason could be that the products were strongly adsorbed on the catalyst [33] and the temperature of 40 °C was not enough to allow desorbing processes. A similar explanation was suggested also by Vardon [23]. Both conversion and selectivity results for each temperature are reported in Table 2.

Following the evolution of products for the reaction performed at 70 °C (Fig. 10), it was observed that the (2E)-2-hexenedioic acid intermediate was present at very low concentration. The (2Z)-2-hexenedioc acid appears to be the main isomer formed and then transformed into AA. Since *trans* isomer is favoured in the presence of a hydrogenation catalysts [17], we assumed that the *cis* interme-

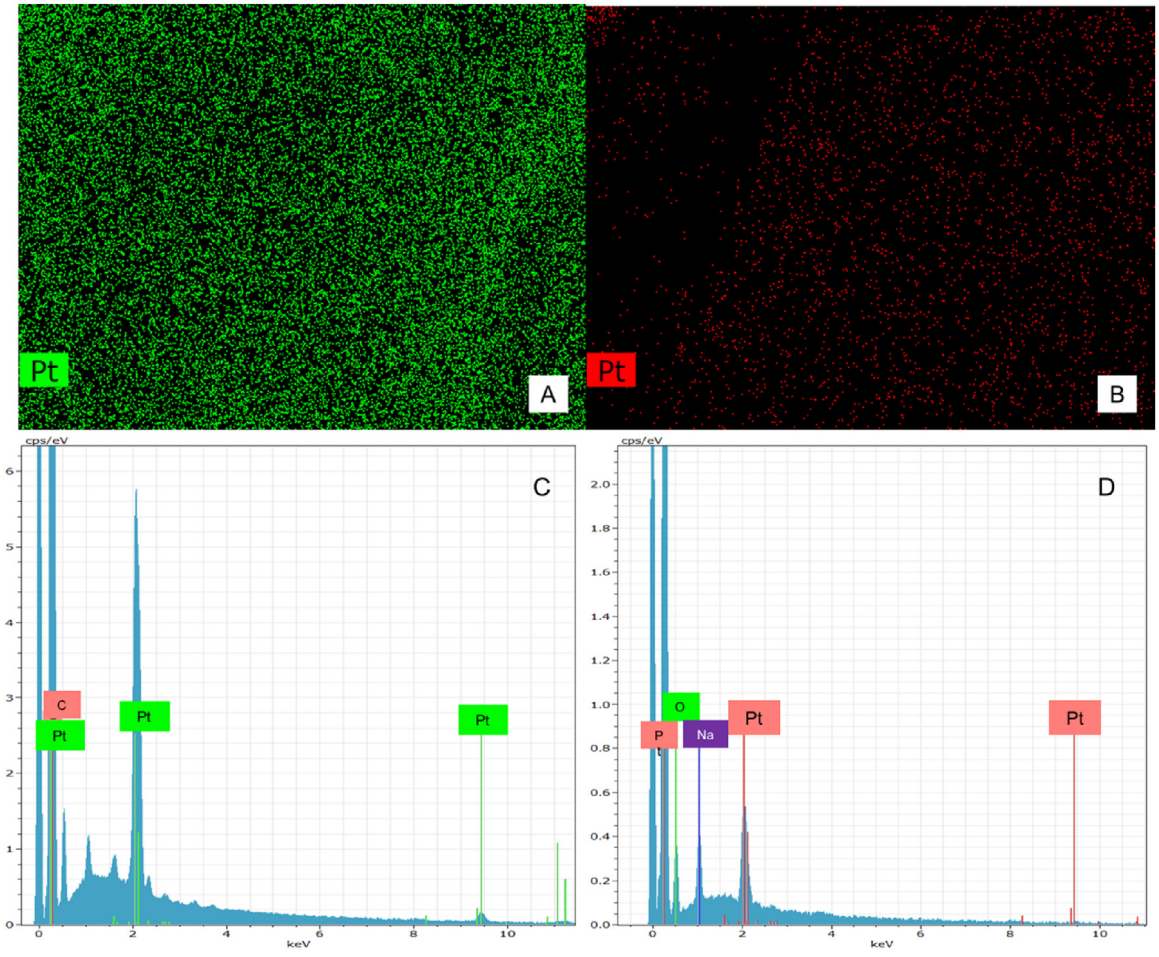

Fig. 8. The energy dispersive X-ray (EDX) mapping analysis of the (A–C) fresh Pt/C 5% catalyst and (B–D) the pre-treated ones.

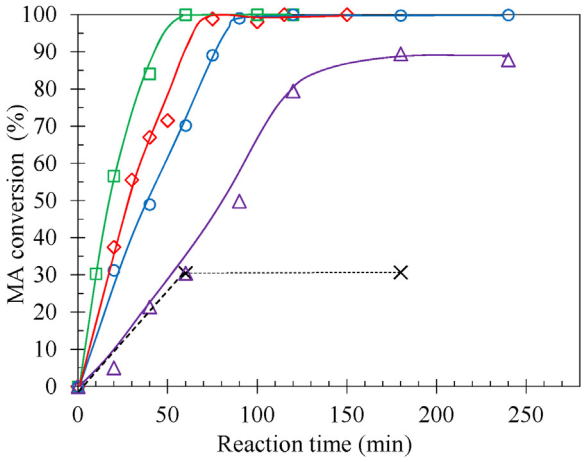

Fig. 9. Sodium *trans,trans*-muconate conversion at (Δ) 40 °C, (○) 50 °C, (◊) 60 °C, (□) 70 °C, (x) and hot filtration at $P(H_2)$ = 4 bar, stirring = 500 rpm, sub/cat = 10 (wt/wt), [MA] = $7 \cdot 10^{-2}$ M.

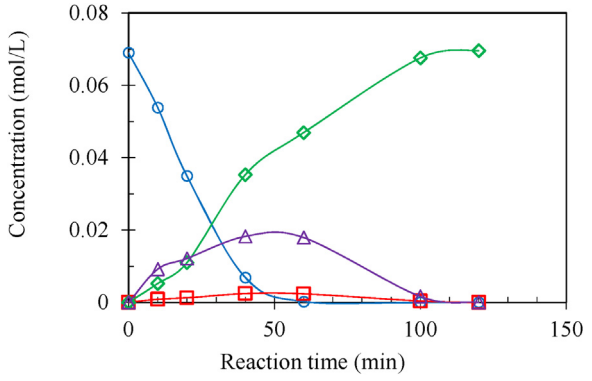

Fig. 10. (○) *trans,trans*-muconic acid, (◊) adipic acid, (□) *cis* and (Δ) *trans* mono-unsaturated intermediates concentration at 70 °C.

diate, during the reaction, isomerizes into the *trans* form, when not completely hydrogenated as depicted in Fig. 11.

By GC/MS analysis it was possible to recognize all the intermediates thus supporting our hypothesized mechanism. *Trans,trans*-MA is hydrogenated to (2E)-2-hexenedioic acid that is further hydrogenated to adipic acid. Isomerization equilibrium between (2E)-2-hexenedioic acid and (2Z)-2-hexenedioc acid can be established, as the last isomer was identified in very low amount. Similarly, the (3E)-3-exenedioic acid, detected in the work of Vardon et al. [23], was detected in traces (<1%).

Recycling tests on the catalyst were performed to obtain information about the stability of the catalyst. The possibility to reuse catalyst is a key point in a further industrial perspective. The test was performed at 70 °C with 10 substrate/catalyst ratio (wt/wt) with 8×10^{-2} M muconate concentration. The catalyst was filtered after 2 h and reused without any further activation step with a fresh solution of MA. Even after 10 cycles, a full conversion of MA and a full selectivity toward adipic acid was obtained after 2 h. The results are reported in Table 3.

Table 2
MA conversion (C) and selectivity (S) toward AA, cis and trans monounsatured intermediates.

Reaction temperature (°C)	Reaction time (min)	$C_{t,tMA}$ (%)	S_{AA} (%)	S_{cis_int} (%)	S_{trans_int} (%)
T = 40 °C	0	0,00	0	0	0
	20	5,00	0	8,8	91,2
	40	21,40	12,3	6,8	80,9
	60	30,50	41,25	5,9	52,85
	90	49,90	58,89	2,6	38,51
	120	79,50	58,6	2,8	38,6
	180	89,50	76,63	2,7	20,67
	240	87,90	77,94	2,4	19,66
T = 50 °C	0	0	0	0	0
	20	31,1	26,3	6,8	66,9
	40	49	44,1	2,5	53,4
	60	70,2	51,5	2,9	45,6
	75	89,1	46,5	5,8	47,7
	90	99,07	62,1	5,1	32,8
	120	100	84,7	3,1	12,2
	180	99,9	100	0	0
	240	100	100	0	0
T = 60 °C	0	0	0	0	0
	20	37,5	33,2	4,3	62,5
	30	55,6	38,2	4,7	57,1
	40	67,1	49,2	5,9	44,9
	50	71,6	55,2	5,7	39,1
	75	98,9	74,6	3,9	21,5
	115	100	100	0	0
	150	100	100	0	0
T = 70 °C	0	0	0	0	0
	10	30,3	58,6	3,3	38,1
	20	56,7	59,4	8,4	32,2
	40	84,1	65,7	3,2	31,1
	60	100	100	0	0
	100	100	100	0	0
	120	100	100	0	0

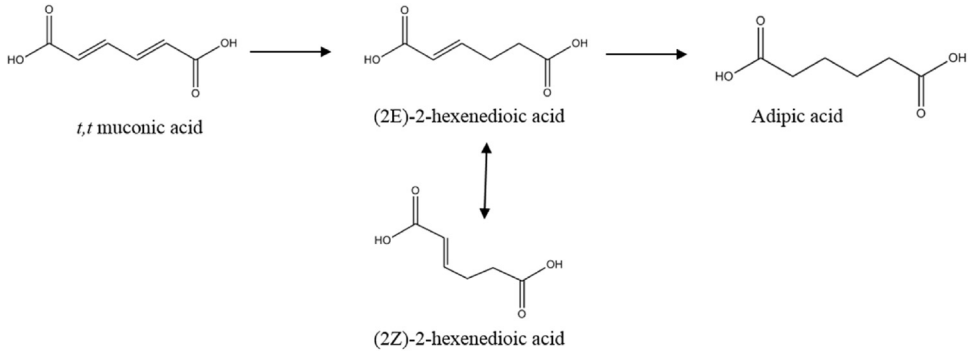

Fig. 11. Hypothesized reaction pathway.

Table 3
Catalyst recycling tests results at $P(H_2) = 4$ bar, stirring = 500 rpm, sub/cat = 10 (wt/wt), $[MA] = 7 \cdot 10^{-2}$ M.

Test #	MA conversion (%)	AA selectivity (%)
1	100	100
2	100	100
3	100	>99
4	>99	>99
5	>99	>99
6	>99	>99
7	>99	>99
8	>99	>99
9	>99	>99
10	>99	>99

Once proven the good performances of the catalyst on *trans,trans* MA, the same hydrogenation conditions were repeated on the *cis,cis* form, with the same good results. However, thinking to the industrial process, a solution with the sole *cis,cis* isomer is unlikely to be found, given the spontaneous rearrangement to the *cis,trans* form in acidic environment. Still, the *cis,cis* form could be preserved, as long as any crystallization step on the fermentation broth is excluded. Consequently, we tried to hydrogenate a synthetic solution, which could mimic the salt buffer of the fermentation, assuming that the broth was previously clarified from the microorganisms and treated by means of ultrafiltration and activated carbon to remove all the biological matter. The results are reported in Fig. 12.

In presence of salt, the reaction is sensibly slower: AA yield after 180 min is only 73%. This result can be explained considering the salts concurrent adsorption on the catalyst surface, and confirms the need to perform the hydrogenation on a substrate with the highest possible purity. This would be beneficial also on the duration of the catalyst, as in absence of the growth support salts the noble metal poisoning would be prevented.

4. Conclusions

This work addressed the production of adipic acid from renewables, focusing on the hydrogenation of muconic acid, an

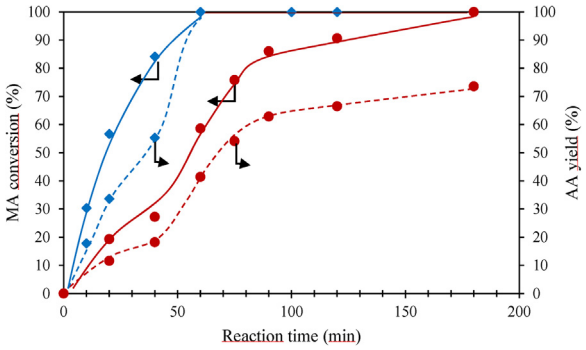

Fig. 12. MA conversion (solid line) and AA selectivity (dashed line) – (○) *cis,cis-MA in* the synthetic salt fermentation broth and (◊) in pure water: P(H_2) = 4 bar, T=70 °C, stirring = 500 rpm.

intermediate achieved by fermentation of lignocellulosic biomass. A novel approach for the hydrogenation study was followed, using the *trans,trans* isomer of MA as a reaction substrate, differently from previous studies where the hydrogenation was performed on *cis,cis*-MA, as produced directly by the microorganisms. *Trans,trans* isomer is the most stable form, hence the optimal hydrogenation conditions for this isomers can be extended also for mixtures of the others. Also, a sole *cis,cis* solution is unlikely to be found in any industrial application, after downstream operations which involve thermal treatments and acid crystallizations.

The first goal of this study was the development of a suitable and robust analytical method for the evaluation of conversion and selectivity toward the different monounsatured intermediates, so to provide also a first insight of the reaction mechanism.

The hydrogenation tests were performed in a batch slurry reactor in kinetic regime using water as a reaction medium. The reaction achieved a complete conversion and total selectivity to AA in less than 90 min, at the low hydrogen pressure of 4 bar and mild temperature as low as 50 °C, paving the way to the scalability of the technology.

Finally, the catalyst was tested also in conditions that mimic a hydrogenation of the pre-treated fermentation broth in the industrial conditions, i.e. an aqueous solution of *cis,cis*-MA in presence of the fermentation buffer salts. As expected, both the MA conversion and AA yield were lower, due to the concurrent adsorption of the ions present in solution on the catalysts surface. This provides a clear indication of the necessity of preliminary purification steps at industrial scale, before the hydrogenation reaction.

Tests on the catalyst recyclability showed the possibility to reuse it up to 10 times without any loss in activity and selectivity. These unprecedented good performances of the catalyst and the efficient analytical method set in this work encourage further studies on MA hydrogenation.

A detailed kinetic study will be performed, to disclose the details of the reaction step, and assess the hypothesized mechanism. Also, new reaction conditions will be explored, passing from the model solutions to substrates derived from real fermentation broths.

The hydrogenation reaction is the last key step for the achievement of green adipic acid, but it was shown that the success of this final transformation is tightly related to the upstream process conditions. The development of novel bio-chemical process requires an integrated and interdisciplinary effort from R&D: this work will possibly give a contribution to accelerate the shift to this novel green solution.

References

[1] J.P. Oppenheim, G.L. Dickerson, Adipic acid, Chem. Technol. (2014) 1–27, http://dx.doi.org/10.1002/0471238961.0104091604012209.a01.pub2.
[2] J.C.J. Bart, S. Cavallaro, Transiting from adipic acid to bioadipic acid. Part II. Biosynthetic pathways, Ind. Eng. Chem. Res. 54 (2) (2015) 567–576.
[3] W. Niu, K.M. Draths, J.W. Frost, Benzene-free synthesis of adipic acid, Biotechnol. Progress 18 (2) (2002) 201–211.
[4] M.H. Thiemens, W.C. Trogler, Nylon production: an unknown source of atmospheric nitrous oxide, Science 251 (1991) 932–934.
[5] K.M. Draths, J.W. Frost, Environmentally compatible synthesis of adipic acid from D-glucose, J. Am. Soc. 116 (1991) 399–400.
[6] T. Polen, M. Spelberg, M. Bott, Toward biotechnological production of adipic acid and precursors from biorenewables, J. Biotechnol. 167 (2) (2013) 75–84.
[7] D.R. Vardon, M.A. Franden, C.W. Johnson, E.M. Karp, M.T. Guarnieri, J.G. Liger, M.J. Salm, T.J. Strathmann, G.T. Beckham, Adipic acid production from lignin, Energy Environ. Sci. 8 (2) (2015) 617–628.
[8] R. Patnaik, J.C. Liao, Engineering of Escherichia coli central metabolism for aromatic metabolite production with near theoretical yield, Appl. Environ. Microbiol. 60 (11) (1994) 3903–3908.
[9] Y. Denga, L. Mac, Y. Mao, Biological production of adipic acid from renewable substrates: current and future methods, Biochem. Eng. J. 105 (2016) 16–26.
[10] N. Xie, H. Liang, R. Huang, P. Xu, Biotechnological production of muconic acid: current status and future prospects, Biotechnol. Adv. 32 (3) (2014) 615–622.
[11] C.W. Johnson, D. Salvachúa, P. Khanna, H. Smith, D.J. Peterson, G.T. Beckham, Enhancing muconic acid production from glucose and lignin-derived aromatic compounds via increased protocatechuate decarboxylase activity, Metab. Eng. Commun. 3 (2016) 111–119.
[12] R. Lu, F. Lu, J. Chen, W. Yu, Q. Huang, J. Zhang, J. Xu, Production of diethyl terephthalate from biomass-derived muconic acid, Angew. Chem. Int. Ed. 55 (2016) 249–253.
[13] J.M. Carraher, T. Pfennig, R.G. Rao, B.H. Shanks, J.-P. Tessonnier, Cis,cis-muconic acid isomerization and catalytic conversion to biobased cyclic-C6-1,4-diacid monomers, Green Chem. (2017), http://dx.doi.org/10.1039/c7gc00658f [Ahead of Print].
[14] S. Mizuno, N. Yoshikawa, M. Seki, T. Mikawa, Y. Imada, Microbial production of cis, cis muconic acid from benzoic acid, Appl. Microbiol. Biotechnol. 28 (1988) 20–25.
[15] N.A. Rorrer, D.R. Vardon, J.R. Dorgan, E.J. Gjersing, G.T. Beckham, Biomass-derived monomers for performance-differentiated fiber reinforced polymer composites, Green Chem. 19 (12) (2017) 2812–2825, http://dx.doi.org/10.1039/c7gc00320j.
[16] J.E. Matthiesen, J.M. Carraher, M. Vasiliu, D.A. Dixon, J.P. Tessonnier, Electrochemical conversion of muconic acid to biobased diacid monomers, Sustainable Chem. Eng. 4 (6) (2016) 3575–3585.
[17] J.E. Matthiesen, M. Suástegui, Y. Wu, M. Viswanathan, Y. Qu, M. Cao, N. Rodriguez-Quiroz, A. Okerlund, G. Kraus, D.R. Raman, Z. Shao, J.-P. Tessonnier, Electrochemical conversion of biologically produced muconic acid: key considerations for scale-up and corresponding technoeconomic analysis, ACS Sustainable Chem. Eng. 4 (2016) 7098–7109.
[18] K.M. Draths, J.W. Frost, Environmentally compatible synthesis of adipic acid from D-glucose, J. Am. Chem. Soc. 116 (1) (1994) 399–400.
[19] J.M. Thomas, R. Raja, B.F.G. Johnson, T.J. O'Connell, G. Sankar, T. Khimyak, Bimetallic nanocatalysts for the conversion of muconic acid to adipic acid, Chem. Commun. (2003) 1126–1127.
[20] V. Bui, M.K. Lau, D. MacRae, D. Schweitzer, (2013) US2013030215A1.
[21] J.W. Frost, A. Miermont, D. Schweitzer, V. Bui, Preparation of trans, trans muconic acid and trans, transmuconates (2010) US 8426639 B2.
[22] X. Li, D. Wu, T. Lu, G. Yi, H. Su, Y. Zhang, Highly efficient chemical process to convert mucic acid into adipic acid and DFT studies of the mechanism of the rhenium-catalyzed deoxydehydration, Angew. Chem. 53 (2014) 4200–4204.
[23] D.R. Vardon, N.A. Rorrera, D. Salvachúa, A.E. Settle, C.W. Johnson, M.J. Menart, N.S. Cleveland, P.N. Ciesielski, K.X. Steirer, J.R. Dorgan, G.T. Beckham, cis,cis-Muconic acid: separation and catalysis to bio-adipic acid for nylon-6,6 polymerization, Green Chem. 18 (2016) 3397–3413.
[24] X. She, H.M. Brown, X. Zhang, B.K. Ahring, Y. Wang, Selective hydrogenation of trans,trans-muconic acid to adipic acid over a titania-supported rhenium catalyst, ChemSusChem 4 (2011) 1071–1073.
[25] S. Scelfo, R. Pirone, N. Russo, Highly efficient catalysts for the synthesis of adipic acid from cis,cis-muconic acid, Catal. Commun. 18 (2016) 98–102.
[26] J.M. Carraher, J.E. Matthiesen, J.P. Tessonnier, Comments on Thermodynamics of cis,cis-muconic acid solubility in various polar solvents at low temperature range, J. Mol. Liq. 224 (2016) 420–422.
[27] C.M. Todaro, H.C. Vogel (Eds.), Fermentation and Biochemical Engineering Handbook, William Andrew, 2014.
[28] P.A. Ramachandran, R.V. Chaudhari, Three Phase Catalytic Reactors, Gordon and Breach Publishers, New York, 1983.
[29] M.V. Rajashekharam, D.D. Nikalje, R. Jaganathan, R.V. Chaudhari, Hydrogenation of 2,4-dinitrotoluene using a Pd/Al2O3 catalyst in a slurry reactor: a molecular level approach to kinetic modeling and nonisothermal effects, Ind. Eng. Chem. Res. 36 (3) (1997) 592–604.
[30] R.V. Chaudhari, C.V. Rode, R.M. Deshpande, R. Jaganathan, T.M. Leib, P.L. Mills, Kinetics of hydrogenation of maleic acid in a batch slurry reactor using a bimetallic Ru–Re/C catalyst, Chem. Eng. Sci. 58 (2003) 627–632.
[31] R.M. Machado, Fundamentals of Mass Transfer and Kinetics for the Hydrogenation of Nitrobenzene to Aniline, ALR Application Note, 2007 (N°01-2007).
[32] J. Hájek, D.Y. Murzin, Liquid-phase hydrogenation of cinnamaldehyde over a Ru–Sn sol–gel catalyst. 1. Evaluation of mass transfer via a combined

experimental/theoretical approach, Ind. Eng. Chem. Res. 43 (2004) 2030–2038.
[33] Y. Sano, N. Yamaguchi, T. Adachi, Mass transfer coefficients for suspended particles in agitated vessels and bubble columns, J. Chem. Eng. Jpn. 7 (4) (1974) 255–261.
[34] J.J. McKetta Jr, Encyclopedia of Chemical Processing and Design (Pumps: Bypass to Reboilers), vol. 46, CRC Press, 1993.
[35] G.J.K. Acres, B.J. Cooper, Carbon-supported platinum metal catalysts for hydrogenation reactions. Mass transport effects in liquid phase hydrogenation over Pd/C, J. Appl. Chem. 22 (1972) 769–785.